

data support the model that assumes the electron spins are polarized only in the discharge region and that after the electrons are trapped in the bubble (outside the high-electric-field discharge region) no further polarization occurs. In ^3He , we propose that not only does polarization take place in the discharge (although this produces only a small fraction of the average polarization) but that spin-lattice relaxation towards steady-state magnetization occurs *when the electron is in the bubble state*.

These new results suggest several experiments which we are attempting. The existence of a strong electron-nuclear interaction might make it possible to observe dynamic nuclear polarization in liquid ^3He . Such studies will give direct confirmation of our explanation of these ESR experiments as well as possibly providing a technique for producing large polarization in an important nuclear-physics target material. The best reported polarization scheme in liquid ^3He , using room-temperature optically pumped gas in contact with liquid at low temperatures, achieved only 0.85% polarization in the steady state.⁵

The ESR spectra of negative ions in ^4He - ^3He mixtures will also be measured. Andreev⁶ and others have predicted a temperature-dependent condensation of the ^3He atoms on the free surface of bulk helium for dilute mixtures of ^3He . Such condensation of the ^3He atoms should also occur on the free surface of the ion bubbles. We believe

our ESR experiments can detect this condensation.

It may also be possible to observe the ESR spectra of ions trapped in solid ^3He . A careful search for the signal in the solid was made in ^4He but none was detected, indicating that in solid ^4He the electronic T_1 is so long that steady-state polarization is extremely small. In solid ^3He , the hyperfine interaction may be sufficiently short to reduce T_1 so that the ESR of these trapped and almost stationary ions can be observed.

The authors gratefully acknowledge the illuminating discussions with and valuable suggestions made by Professor Arnold J. Dahm. This research was supported by the National Science Foundation under Grant No. 1679B.

^(a)Permanent address: Department of Physics, SUNY at Buffalo, Amherst, N. Y. 14260.

^(b)Present address: Schlumberger Well Services, Houston, Tex. 77001.

¹P. H. Zimmermann, J. F. Riechert, and A. J. Dahm, Phys. Rev. B **15**, 2630 (1977).

²The signal amplitudes are normalized per unit current.

³A few milliseconds is a typical transit time for these ions.

⁴V. Celli, M. Cohen, and M. J. Zuckerman, Phys. Rev. **173**, 253 (1968).

⁵H. H. McAdams, Phys. Rev. **170**, 276 (1968).

⁶A. F. Andreev, Zh. Eksp. Teor. Fiz. **50**, 1415 (1966) [Sov. Phys. JETP **23**, 939 (1966)].

Orientation Dependence of Core Edges in Electron-Energy-Loss Spectra from Anisotropic Materials

R. D. Leapman and J. Silcox

School of Applied and Engineering Physics, Cornell University, Ithaca, New York 14853

(Received 4 December 1978)

We have investigated the orientation dependence of the structure near the boron K edge in electron-energy-loss spectra from hexagonal boron nitride. Angular distributions of spectra recorded from crystals with c axis tilted at 45° to the beam allow us to determine unambiguously the π and σ character of the final states at different energies. Results are in quantitative agreement with a model based on hybridized atomic orbitals.

In this Letter, we report the observation of an orientational dependence of core-edge fine structure in electron-energy-loss spectra of thin anisotropic crystals. Fine structure can arise when an inner-shell electron in a state $|i\rangle$ makes a transition to an unoccupied state $|f\rangle$ characterized by a high combined value of density of states and matrix element factors and accompanied by

a momentum transfer $\vec{q} = q\vec{\epsilon}_q$.¹⁻⁵ At the small scattering angles considered here ($q \lesssim 0.6 \text{ \AA}^{-1}$), the cross section for this process will depend on matrix elements which can be put in the dipole form $q\langle f | \vec{\epsilon}_q \cdot \vec{r} | i \rangle$. The implied angular dependence can therefore be explored by measurement of energy-loss spectra for $\vec{\epsilon}_q$ parallel to different directions in the crystal, thus giving the orienta-

tion of the final state $|f\rangle$. In the present experiments, such spectra for the boron K edge in hexagonal boron nitride are measured and used to verify the character and energy of unoccupied π and σ valence states. In the form just given above, the matrix element is similar to the photoelectric matrix element with $\vec{\epsilon}_q$ playing the role of the polarization unit vector. Thus the experiments are similar to studies with polarized synchrotron radiation of an equivalent energy, as reported for layered chalcogenides⁶ and boron nitride.⁷ Our observations are substantially different from the x-ray observations on BN and are therefore of some interest in that regard. Moreover, the experiments are the first explicit demonstration in detail that this type of study can be performed with fast electrons.

Within the dipole approximation, the differential cross section with respect to energy loss E and solid angle Ω can be given in the form⁸

$$\frac{d^2\sigma(\theta)}{dE d\Omega} = \frac{4}{a_0^2 q^2} |\langle f | \vec{\epsilon}_q \cdot \vec{r} | i \rangle|^2, \quad (1)$$

where a_0 is the Bohr radius and $|f\rangle$ is normalized per unit energy. We are interested in the angular dependence of the cross section with scattering geometry as sketched in Fig. 1(a). For small scattering angles θ , the dipole selection rules must be satisfied for the change in angular momentum ($\Delta l = \pm 1$), so that for an initial $|1s\rangle$ state, the final state has $l=1$ symmetry. Since BN is an insulator, a tight-binding model for the final states made up of $2s$ and $2p$ orbitals is a common first approximation.⁹ Because of the small spatial extent of the initial-state wave function, the dominant contribution to the matrix element is overlap between the initial state and that part of the tight-binding $|f\rangle$ representing the atomic state localized on the same atom. We therefore will neglect contributions to the matrix element from atomic states in $|f\rangle$ localized on the other atoms. The model is essentially atomic but we note that band-structure effects will be reflected in the energy level of the final state and the corresponding density of states. These will determine the energy dependence of the spectrum above the core edge whereas the angular part of the matrix element will determine the dependence on scattering angle. In a crystal the lobes of the angular parts of the wave functions are determined by the structure. Thus in BN an appropriate sum of empty $2p_z$ states parallel to the c axis represents π^* antibonding orbitals and hybridized $2s p_x p_y$ states perpendicular to the c axis repre-

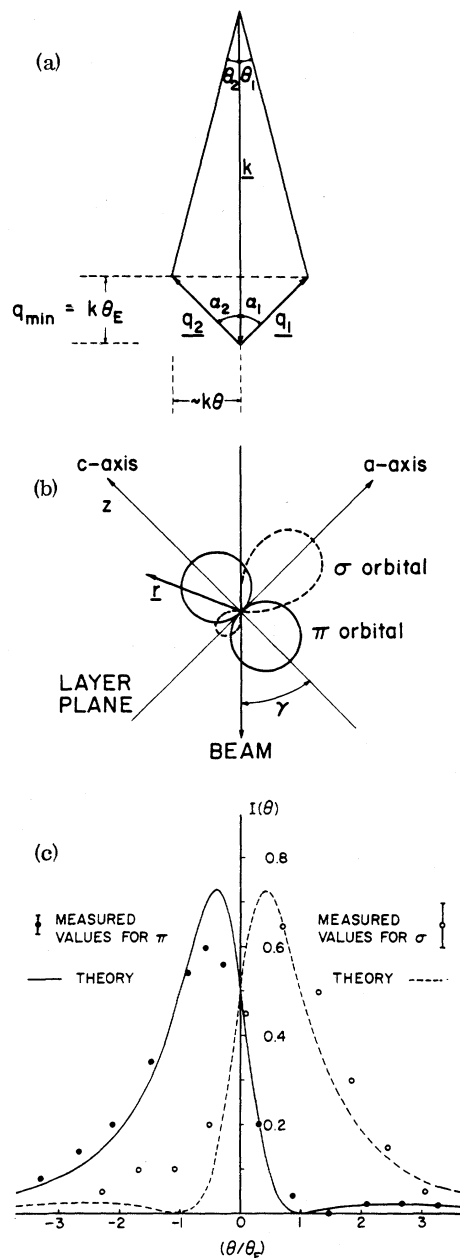


FIG. 1. (a) Diagram for scattering through angle $\theta = \theta_E$ for incident electron momentum \vec{k} and momentum transfer \vec{q} . Subscripts 1 and 2 correspond to $+\theta$ and $-\theta$, respectively. The parallel (minimum) and perpendicular q values are indicated. (b) Schematic diagram of BN tilted at $\gamma = -45^\circ$ to c axis. The position coordinate \vec{r} is shown. (c) Theoretical and experimental angular distributions for the $1s \rightarrow \pi$ and $1s \rightarrow \sigma$ transitions.

sent antibonding σ^* orbitals. This is shown schematically in Fig. 1(b) where the electron beam is incident at an angle γ to the c axis.

If we define the angle between the c axis and

ξ_q as α , then evaluation of the angular part of Eq. (1) for the π^* orbital gives

$$d^2\sigma(\theta)/dE d\Omega = q^{-2}f(E) \cos^2(\alpha - \gamma) \\ \propto (\theta^2 + \theta_E^2)^{-1} \cos^2[\tan^{-1}(\theta/\theta_E) - \gamma], \quad (2)$$

where $\theta_E = E/2E_0$ (with E_0 the incident energy) arises from standard scattering kinematics [Fig. 1(a)]. The radial integral, the energy dependence, and the density of states are factored out in the term $f(E)$. A similar calculation for the σ^* orbital gives

$$d^2\sigma(\theta)/dE d\Omega \propto (\theta^2 + \theta_E^2)^{-1} \sin^2[\tan^{-1}(\theta/\theta_E) - \gamma]. \quad (3)$$

For a value of $\gamma = -45^\circ$ the numerators in Eqs. (2) and (3) are peaked at $-\theta_E$ for the π^* orbital corresponding to ξ_q parallel to the c axis, and at $+\theta_E$ for the σ^* orbital when ξ_q is parallel to the a axis. Division by q^2 shifts the maxima to $+0.41\theta_E$; this is shown in Fig. 1(c) where the relation between the scattering distributions and the orientations of the orbitals in Fig. 1(b) is evident.

Fine structure in the $1s$ core excitation spectrum of hexagonal BN and graphite has been reported previously for electrons incident parallel to the c axis.^{2-4,10} In the case of graphite, a very sharp peak at the edge has been attributed to excitation of π^* states, whereas a broader peak about 7 eV above threshold has been attributed to a $1s \rightarrow \sigma^*$ transition.³ This identification has been carried out by comparison of spectra with the density of states derived from band calculations. It is consistent with existing momentum-dependence studies on graphite at normal incidence.¹⁰ As presented in the previous paragraph, comparison of the cross sections on either side of $\theta=0$ for electrons incident at 45° to the c axis will determine unambiguously the final-state π^* or σ^* orbital character of these peaks. It is necessary to probe the scattering on an angular scale commensurate with θ_E , which for the boron K edge at 190 eV and 75 keV incident energy has the value 1.3×10^{-3} rad (or 0.2 \AA^{-1} perpendicular momentum transfer). An angular resolution of order 2×10^{-4} rad is therefore desirable to explore the effect.

These conditions are readily achievable in electron-microscope-electron-spectrometer system described previously.¹¹ In using this electron microscope in the selected-area diffraction mode, a $4\text{-}\mu\text{m}$ spot of 75-keV electrons is incident on the specimen with a beam divergence of $\sim 2 \times 10^{-4}$ rad. The diffraction pattern is viewed on a fluorescent screen (and recorded on photographic

plates) with the specimen inserted in a special holder at 45° to obtain the geometry in Fig. 1(b). An entrance slit to the spectrometer selects electrons according to the angle of scattering and the spectrometer disperses them in a direction perpendicular to the slit. A two-dimensional pattern results giving a map of the scattered electron intensity as a function of both energy loss and scattering angle. The optical density of a photographic plate exposed appropriately to the electrons is to a good approximation linear with the electron intensity and profiles can be obtained with a densitometer. Samples were prepared by grinding bulk BN and suspending the powder in ethyl alcohol. The powder was picked up on a support film of 100- \AA amorphous carbon and, after drying, flakes about $3 \mu\text{m}$ in diameter lying flat on the substrate were selected for study. Calibration of scattering angles was carried out using the diffraction pattern and energy loss using a digital offset to the Wien filter. Absolute measurement of the energy losses was accurate to $\sim \pm 0.5$ eV and spectra were recorded at an energy resolution of ~ 1.4 eV.

In the region of the boron K edge of a sample 200–300 \AA thick, tilted at 45° , three peaks can be identified. Following earlier work on graphite, a strong peak at 192 eV can be attributed to the $1s \rightarrow \pi^*$ band transitions. Peaks at 199 and 204.5 eV can be attributed to the $1s \rightarrow \sigma^*$ band transitions. The change in shape of the spectrum with scattering angle is shown in Fig. 2 where densitometer traces have been recorded at $\theta=0$, ± 1.2 , and ± 2.4 mrad. For $-\theta$ the π peak is strong and the σ peaks are weak, while for $+\theta$ the situation is reversed as expected. Angular scans recorded with a resolution of $\sim 2 \times 10^{-4}$ rad are shown in Fig. 1(c). These measured values were obtained from densitometer traces after subtraction of the background intensity immediately preceding the peaks and scaling to facilitate comparison with theory. Agreement with the theoretical curve is good for the π peak and even the drop to zero intensity at $\sim \theta_E$ is predicted followed by a secondary maximum at $\sim 2.4\theta_E$ whose intensity is only about 3% of the main maximum at $\sim -0.4\theta_E$. Agreement is also reasonable for the σ peak, and the lack of a secondary maximum here may be accounted for by the poorer statistics and by some multiple scattering. It is noted that the total specimen thickness ($\sim 300 \text{ \AA}$) as estimated from the low-loss spectrum is not great enough to produce appreciable multiple scattering in the region of the boron K edge. The similar angular depen-

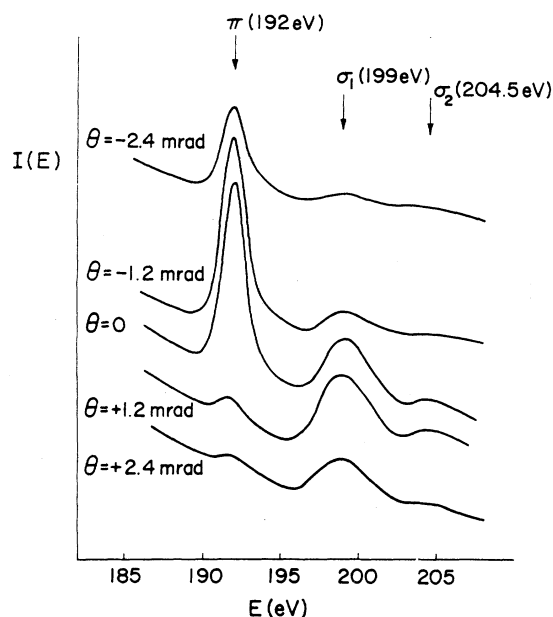


FIG. 2. Spectrum in region of boron K edge at different values of θ showing changes in amplitude of the π and σ peaks for a sample tilted at 45° to the c axis.

dence of the peaks at 199 and 204.5 eV (Fig. 2) allows us to characterize both as $1s \rightarrow \sigma^*$ transitions which we label as σ_1 and σ_2 , respectively.

The photoelectric absorption observations of Brown, Backrach, and Skibowski⁷ over an energy range between 186 and 201 eV are difficult to reconcile with our observations. A peak at 192 eV reported by these authors increases little or not at all for the two crystal orientations investigated. Another peak occurs in their data at 195 eV polarized parallel to the c axis. We also see a faint peak at this energy in our normal-incidence data but it is very weak compared with the strong 192-eV peak which we find is also polarized along the c axis. A number of theoretical band-structure calculations of BN have been performed^{9,12,13} and all these predict a final density of states at the Brillouin-zone boundary QP with peaks from the unoccupied π^* band lower in energy than the peaks from the two σ^* bands. Such calculations are consistent with our measurements but excitonic effects including electronic relaxation near the core hole should not be ignored. These can shift peaks in the region of the core edge towards lower energies and modify their shapes.¹⁴ It seems unlikely that these shifts will change the sequence of π^* and σ^* peaks separated by the order of 7 eV. At present we do not make a detailed comparison of our data with the ground-

state density of states but emphasize that our orientation dependence studies can determine final-state symmetries. Although the reasons for the discrepancies between our data and the synchrotron studies are not clear, we note that some difficulties have previously been encountered with x-ray polarization measurements. Results of an experiment on the Se L edge originally attributed to a polarization dependence¹⁵ were later shown to arise from holes in the sample.⁶

Our angular studies at different crystal orientations permit separation of the peaks into those associated with the π^* and σ^* states, respectively, since they provide unambiguous identification of the orientation of the $l=1$ part of the final states. We add that measurements made on BN at normal incidence also agree with theory and these results together with data for graphite will be published separately. For low- Z elements, in particular, this promises to provide a useful addition to the probes of electronic structure currently available.

We are indebted to Dr. P. L. Fejes for his experimental assistance. Financial support from the National Science Foundation through the Cornell University Materials Science Center is gratefully acknowledged.

¹M. S. Isaacson, *J. Chem. Phys.* **56**, 1813 (1972).

²C. Colliex and B. Jouffrey, *Philos. Mag.* **25**, 491 (1972).

³R. F. Egerton and M. J. Whelan, *J. Electron Spectrosc.* **3**, 232 (1974).

⁴C. J. Roussouw, R. F. Egerton, and M. J. Whelan, *Vacuum* **26**, 427 (1977).

⁵J. J. Ritsko, N. O. Lipari, P. C. Gibbons, and S. E. Schnatterly, *Phys. Rev. Lett.* **37**, 1068 (1976).

⁶S. M. Heald and E. A. Stern, *Phys. Rev. B* **16**, 5549 (1977).

⁷F. C. Brown, R. Z. Bachrach, and M. Skibowski, *Phys. Rev. B* **13**, 2633 (1976).

⁸H. A. Bethe, *Ann. Phys. (Paris)* **5**, 325 (1930).

⁹A. Zunger, A. Katzir, and A. Halperin, *Phys. Rev. B* **13**, 5560 (1976).

¹⁰B. M. Kincaid, A. E. Meixner, and P. M. Platzman, *Phys. Rev. Lett.* **40**, 1296 (1978).

¹¹G. H. Curtis and J. Silcox, *Rev. Sci. Instrum.* **42**, 630 (1971).

¹²M. S. Nakhmanson and V. P. Smirnov, *Fiz. Tverd. Tela* **13**, 2388 (1971) [*Sov. Phys. Solid State* **13**, 2763 (1972)].

¹³E. Doni and G. Pastori Parravicini, *Nuovo Cimento* **63B**, 117 (1969).

¹⁴E. J. Mele and J. J. Ritsko, to be published.

¹⁵E. A. Stern, D. E. Sayers, and F. W. Lytle, *Phys. Rev. Lett.* **37**, 298 (1976).